minerals

MDPI

Article

Nöggerathite-(Ce), $(Ce,Ca)_2Zr_2(Nb,Ti)(Ti,Nb)_2Fe^{2+}O_{14}$, a New Zirconolite-Related Mineral from the Eifel Volcanic Region, Germany

Nikita V. Chukanov [1,*], Natalia V. Zubkova [2], Sergey N. Britvin [3,4], Igor V. Pekov [2,5], Marina F. Vigasina [2], Christof Schäfer [6], Bernd Ternes [7], Willi Schüller [8], Yury S. Polekhovsky [3], Vera N. Ermolaeva [9] and Dmitry Yu. Pushcharovsky [2]

1 Institute of Problems of Chemical Physics, Russian Academy of Sciences, Chernogolovka, 142432 Moscow, Russia
2 Faculty of Geology, Moscow State University, Vorobievy Gory, 119991 Moscow, Russia; n.v.zubkova@gmail.com (N.V.Z.); igorpekov@mail.ru (I.V.P.); vigasina55@mail.ru (M.F.V.); dmitp@geol.msu.ru (D.Y.P.)
3 Institute of Earth Sciences, St Petersburg State University, Universitetskaya Nab. 7/9, 199034 St Petersburg, Russia; sbritvin@gmail.com (S.N.B.); yury1947@mail.ru (Y.S.P.)
4 Nanomaterials Research Center, Kola Science Centre, Russian Academy of Sciences, Fersman str. 14, 184209 Apatity, Murmansk, Russia
5 Vernadsky Institute of Geochemistry and Analytical Chemistry, Russian Academy of Sciences, Kosygin str. 19, 119991 Moscow, Russia
6 Gustav Stresemann-Strasse 34, 74257 Untereisesheim, Germany; mspech612@gmail.com
7 Bahnhofstrasse 45, 56727 Mayen, Germany; ternes-mayen@web.de
8 Im Straußenpesch 22, 53518 Adenau, Germany; maschwisch@web.de
9 Institute of Experimental Mineralogy, Russian Academy of Sciences, Chernogolovka, 142432 Moscow, Russia; cvera@mail.ru
* Correspondence: chukanov@icp.ac.ru; Tel.: +7-4965221556

Received: 7 September 2018; Accepted: 3 October 2018; Published: 12 October 2018

Abstract: The new mineral nöggerathite-(Ce) was discovered in a sanidinite volcanic ejectum from the Laach Lake (Laacher See) paleovolcano in the Eifel region, Rhineland-Palatinate, Germany. Associated minerals are sanidine, dark mica, magnetite, baddeleyite, nosean, and a chevkinite-group mineral. Nöggerathite-(Ce) has a color that ranges from brown to deep brownish red, with adamantine luster; thel streak is brownish red. It occurs in cavities of sanidinite and forms long prismatic crystals measuring up to 0.02 × 0.03 × 1.0 mm, with twins and random intergrowths. Its density calculated using the empirical formula is 5.332 g/cm^3. The Vickers hardness number (VHN) is 615 kgf/mm^2, which corresponds to a Mohs' hardness of 5½. The mean refractive index calculated using the Gladstone–Dale equation is 2.267. The Raman spectrum shows the absence of hydrogen-bearing groups. The chemical composition (electron microprobe holotype/cotype in wt %) is as follows: CaO 5.45/5.29, MnO 4.19/4.16, FeO 7.63/6.62, Al_2O_3 0.27/0.59, Y_2O_3 0.00/0.90, La_2O_3 3.17/3.64, Ce_2O_3 11.48/11.22, Pr_2O_3 1.04/0.92, Nd_2O_3 2.18/2.46, ThO_2 2.32/1.98, TiO_2 17.78/18.69, ZrO_2 27.01/27.69, Nb_2O_5 17.04/15.77, total 99.59/99.82, respectively. The empirical formulae based on 14 O atoms per formula unit (*apfu*) are: $(Ce_{0.59}La_{0.165}Nd_{0.11}Pr_{0.05})_{\Sigma 0.915}Ca_{0.82}Th_{0.07}Mn_{0.50}Fe_{0.90}Al_{0.045}Zr_{1.86}Ti_{1.88}Nb_{1.07}O_{14}$ (holotype), and $(Ce_{0.57}La_{0.19}Nd_{0.12}Pr_{0.05}Y_{0.06})_{\Sigma 0.99}Ca_{0.79}Th_{0.06}Mn_{0.49}Fe_{0.77}Al_{0.10}Zr_{1.89}Ti_{1.96}Nb_{1.00}O_{14}$ (cotype). The simplified formula is $(Ce,Ca)_2Zr_2(Nb,Ti)(Ti,Nb)_2Fe^{2+}O_{14}$. Nöggerathite-(Ce) is orthorhombic, of the space group *Cmca*. The unit cell parameters are: a = 7.2985(3), b = 14.1454(4), c = 10.1607(4) Å, and V = 1048.99(7) Å^3. The crystal structure was solved using single-crystal X-ray diffraction data. Nöggerathite-(Ce) is an analogue of zirconolite-3*O*, ideally $CaZrTi_2O_7$, with Nb dominant over Ti in one of two octahedral sites and *REE* dominant over Ca in the eight-fold coordinated site. The strongest lines of the powder X-ray diffraction pattern (d, Å (I, %) (*hkl*)) are: 2.963 (91) (202), 2.903 (100) (042), 2.540 (39) (004), 1.823 (15) (400), 1.796 (51) (244), 1.543 (20) (442), and 1.519 (16) (282),

respectively. The type material is deposited in the collections of the Fersman Mineralogical Museum of the Russian Academy of Sciences, Moscow, Russia (registration number 5123/1).

Keywords: nöggerathite-(Ce); new mineral; zirconolite; laachite; sanidinite; crystal structure; alkaline volcanic rock; Laacher See; Eifel

1. Introduction

Zirconolite-related Ca-*REE*-Zr-Ti-Nb oxides have been described in numerous publications as advanced materials suitable for the immobilization of actinides, which are components of high-level radioactive waste [1–5]. Natural zirconolites and related minerals (zirconolite-3*O* $(Ca,REE)_2Zr_2(Ti,Nb)_3FeO_{14}$, zirconolite-3*T* $(Ca,REE)_2Zr_2(Ti,Nb)_3FeO_{14}$, zirconolite-2*M* $(Ca,REE)_2Zr_2(Ti,Nb)_3FeO_{14}$, laachite $Ca_2Zr_2Nb_2TiFeO_{14}$, stefanweissite $(Ca,REE)_2Zr_2(Nb,Ti)(Ti,Nb)_2Fe^{2+}O_{14}$ (IMA 2018-020) and the here-described nöggerathite-(Ce)) are characterized by a wide compositional diversity and can be considered as prototypes of such materials. These minerals usually contain uranium and thorium, the total content of which can reach 15–20 wt % [6]. As a result of exposure to alpha radiation, most such samples are X-ray amorphous, metamict. Some exceptions are crystalline samples of zirconolite-type minerals from young volcanic rocks [7–10].

This paper describes **nöggerathite-(Ce)**, a new zirconolite-related mineral species from the Laach Lake area situated in the Eifel paleovolcanic region, Germany. This mineral is non-metamict because of the very young geological age of the mother rock [11,12].

The root name of the new mineral is given in honor of Johann Jacob Nöggerath (1788–1877), a prominent German mineralogist and geologist. From 1818 Nöggerath was a professor of mineralogy and geology at the University of Bonn. Among his publications is a geological description of the Laach Lake (Laacher See) paleovolcanic region. The Levinson's modifier -(Ce) in the mineral name reflects the predominance of Ce among rare earth elements, which together are dominant in one structure position. The mineral and its name have been approved by the Commission on New Minerals, Nomenclature and Classification of the International Mineralogical Associatiob (IMA number 2017-107). The type material is deposited in the collections of the Fersman Mineralogical Museum of the Russian Academy of Sciences, Moscow, Russia (registration number 5123/1).

2. Materials and Methods

The new mineral was found in the In den Dellen (Zieglowski) pumice quarry, 1.5 km to the notrheast of Mendig, in the Laach Lake (Laacher See) paleovolcano of the Eifel region, Rhineland-Palatinate, Germany. Two specimens have been investigated and considered as the holotype and the cotype, which are fragments of the same sanidinite volcanic ejectum. Associated minerals are sanidine, dark mica, magnetite, baddeleyite, nosean, and a chevkinite-group mineral.

The origin of sanidinites of the Laacher See area has been discussed earlier [9,12–14]. These rocks are derivatives of different foyaite magmas which are comagmatic with haüyne-bearing rocks (haüyne foyaite, haüyne syenite, haüyne monzonite, etc.), or with noseane–cancrinite–nepheline syenites. Sanidinites of the latter type are enriched in rare element (Nb, Zr, *REE*, U, Th) accessory minerals. These rocks are cogenetic with the phonolitic host magma, and the crystallization took place in an intrusive syenite–carbonatite complex at temperatures below 700 °C in the host rock surrounding the top of the magma chamber 5000 to 20,000 years prior to the eruption of the magma chamber [12]. Most probably, nöggerathite-(Ce) and associated minerals forming crystals on the walls of cavities in sanidinite crystallized from above-critical fluid.

Chemical analyses (five for the holotype and three for the cotype) were carried out using an Oxford INCA Wave 700 electron microprobe (WDS mode, 20 kV, 600 pA, 300-nm beam diameter,

Oxford Instruments plc, London, UK) housed at the Institute of Experimental Mineralogy RAS. The counting time per peak was 100 s.

The Raman spectrum of a randomly oriented nöggerathite-(Ce) crystal was obtained on the cotype sample using an EnSpectr R532 spectrometer based on an OLYMPUS CX 41 microscope coupled with a diode laser (λ = 532 nm) at room temperature (Enhanced Spectrometry, San Jose, USA). The spectrum was recorded in the range from 100 to 4000 cm^{-1} with a diffraction grating (1800 mm^{-1}) and spectral resolution of about 6 cm^{-1}. The output power of the laser beam was about 9 mW. The diameter of the focal spot on the sample was less than 10 μm. The backscattered Raman signal was collected with a 40× objective; thel signal acquisition time for a single scan of the spectral range was 2 s, and the signal was averaged over 100 scans.

The Raman spectrum of an oriented laachite crystal used for comparison was obtained with a HORIBA instrument based on the OLYMPUS BX 41/51 microscope (HORIBA Jobin Yvon, Bensheim Germany) with a diode laser (λ = 532 nm) at room temperature. The power of the laser beam at the sample was about 1.5 mW. The spectrum was recorded in a range from 100 to 3800 cm^{-1}, with a diffraction grating (1800 mm^{-1}) and spectral resolution of about 1 cm^{-1}. The diameter of the focal spot on the sample was less than 7 μm. The backscattered Raman signal was collected with 50× objective; signal acquisition time for a single scan of the spectral range was 10 s and the signal was averaged over five scans.

Both Raman spectrometers were housed at Moscow State University.

Maximal and minimal reflectance values (R_{max}/R_{min}) were measured in air using a MSF-21 micro-spectrophotometer (LOMO company, St. Petersburg, Russia) with a monochromator slit width of 0.4 mm and beam diameter of 0.1 mm. SiC (reflection standard 474251, number 545, Jena, Germany) was used as a standard. The spectrophotometer was housed at St. Petersburg State University.

Powder X-ray diffraction data were collected using a Rigaku RAXIS Rapid II diffractometer (Rigaku Corporation, Tokyo, Japan) with a curved image plate detector and rotating anode in Debye–Scherrer geometry, with an accelerating voltage of 40 kV, current of 15 mA, and exposure time 15 min. The distance between sample and detector was 127.4 mm. Data processing was carried out using osc2xrd software [15]. The diffractometer was housed at St. Petersburg State University.

The single-crystal X-ray diffraction experiment was carried out using a Bruker Kappa APEX DUO CCD diffractometer (Bruker AXS GmbH, Karlsruhe, Germany). The diffractometer was housed at Moscow State University. Experimental details are given in Table 1.

Table 1. Crystal data, data collection information and structure refinement details for the holotype specimen of nöggerathite-(Ce).

Characteristics	Data and Methods
Crystal sizes, mm	0.01 × 0.01 × 0.10
Temperature, K	293(2)
Radiation and wavelength, Å	Mo$K\alpha$; 0.71073
F_{000}	1530
θ range for data collection, °	2.88–26.98
h, *k*, *l* ranges	–9 → 7, –18 → 18, –12 → 12
Reflections collected	4962
Independent reflections	617 (R_{int} = 0.0215)
Independent reflections with $I > 2\sigma(I)$	574
Data reduction	Bruker SAINT
Structure solution	Direct methods
Refinement method	Full-matrix least-squares on F^2
Weighting coefficients *a*, *b*	0.0251, 7.1886
Number of refined parameters	71
Final *R* indices (with $I > 2\sigma(I)$)	R_1 = 0.0198, wR_2 = 0.0518
R indices (with all data)	R_1 = 0.0224, wR_2 = 0.0550
GoF	1.161
Largest diffraction peak and hole, e/Å^3	1.53 and –0.70

3. Results

3.1. General Appearance and Mechanical Properties

Nöggerathite-(Ce) forms prismatic crystals measuring up to 0.1 × 0.1 × 1.0 mm, elongated along (001), and simple twins, isolated or combined in random aggregates (Figure 1a,b) in cavities in sanidinite. The main observed crystal forms are pinacoids {100} and {010}, as well as prisms {110} and {120}. The other forms are {111} and minor {001}. In most cases, the twinning plane is (130); thel angle between the *c* axes of the twin components is 65°. The exception is a growth (possibly a twin) with the angle between the *c* axes of the twin components of 90° (Figure 1c). Some crystals of nöggerathite-(Ce) are embedded in sanidine.

The new mineral is translucent to transparent, with a color ranging from brown to very dark reddish brown, almost black, with adamantine luster. The streak is brownish red.

Nöggerathite-(Ce) is brittle with uneven fractures; no cleavage was observed. Hardness, as determined by the micro-indentation method (Vickers hardness number (VHN) load of 20 g), is equal to 615 kgf/mm^2 which corresponds to a Mohs' hardness of $5\frac{1}{2}$. The density calculated using the empirical formula is 5.332 g/cm^3.

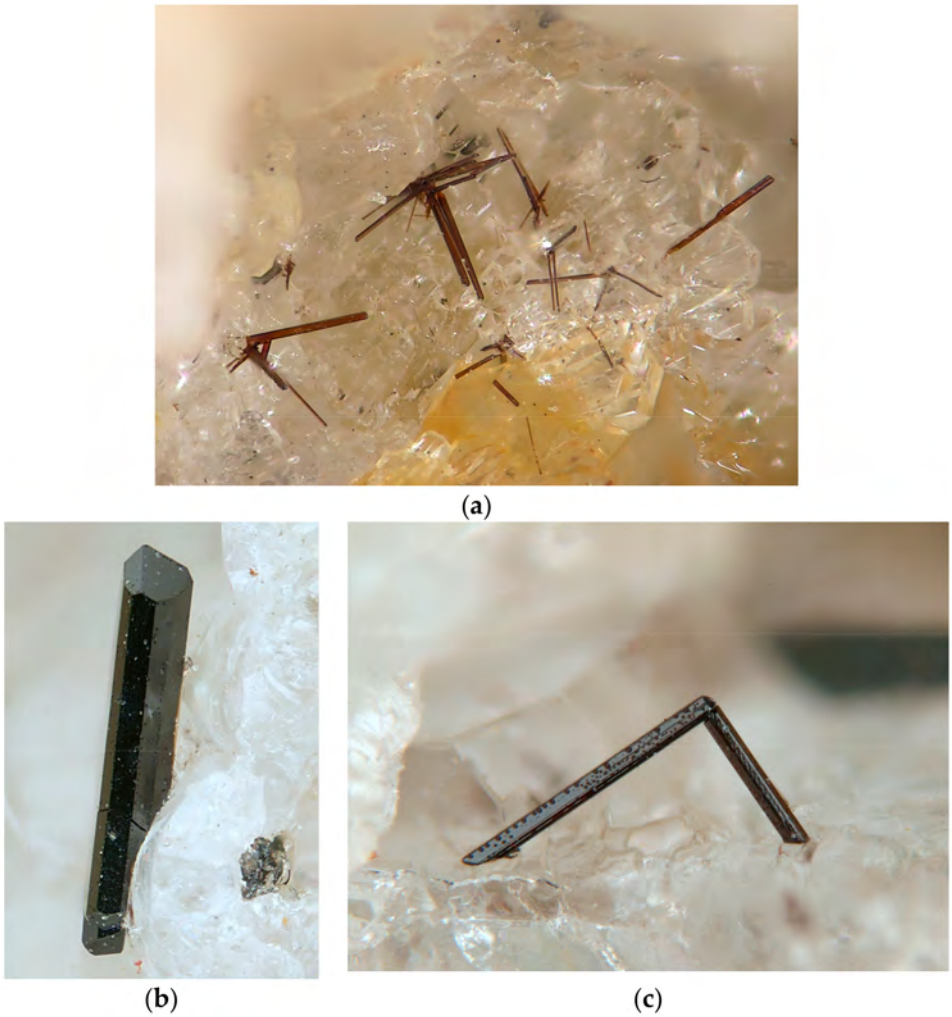

Figure 1. (**a**) Aggregates of brown nöggerathite-(Ce) crystals on sanidine. Photographer: Stefan Wolfsried. Field width: 4 mm; (**b**) Nöggerathite-(Ce) crystal on sanidine. Photographer: Marko Burkhardt. Field width: 0.5 mm; (**c**) Twin of nöggerathite-(Ce) on sanidine. Photographer: Marko Burkhardt. Field width: 1 mm.

3.2. Raman Spectroscopy

The Raman spectrum of nöggerathite-(Ce) (Figure 2) shows the absence of absorption bands of H_2O molecules, OH groups, and CO_3^{2-} anions. The bands in the range of 400–800 cm^{-1} correspond to (Ti,Nb,Zr)–O-stretching vibrations, and the bands in the range of 100–400 cm^{-1} are due to (*REE*,Ca)–O-stretching and O–(Ti,Nb,Zr)–O bending vibrations. Broad features above 900 cm^{-1} in the Raman spectrum of nöggerathite-(Ce) correspond to luminescence due to high amounts of *REE*.

In Raman spectra of laachite (Figure 3), which is a mineral related to nöggerathite-(Ce) but is characterized by much lower *REE*:Ca and Ti:Nb ratios, the bands of (*REE*,Ca)–O- and (Ti,Nb,Zr)–O-stretching vibrations are shifted towards higher and lower values, respectively. This regularity is in accordance with mean masses of corresponding groups of atoms.

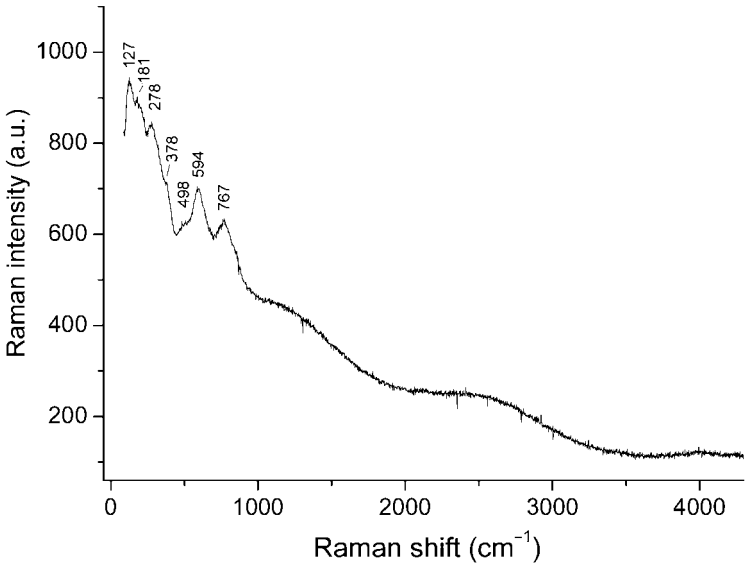

Figure 2. Raman spectrum of nöggerathite-(Ce) (a.u. = arbitrary units).

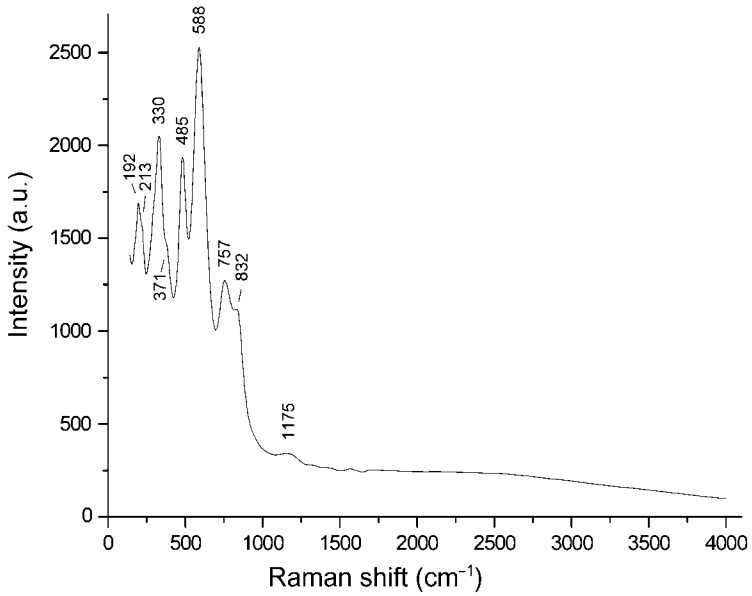

Figure 3. Raman spectrum of laachite $Ca_2Zr_2Nb_2TiFeO_{14}$ obtained with the polarization of the laser beam parallel to the *a* axis of the crystal [9].

3.3. Optical Properties

In reflected light, nöggerathite-(Ce) is optically anisotropic, with ΔR_{589} = 1.27%. The color is light grey, with reddish brown internal reflections. The reflectance values in the visible range are given in Table 2. Mean refractive index calculated from the Gladstone–Dale equation is 2.267.

Table 2. Reflectance values (R_{max}/R_{min}) for nöggerathite-(Ce). Reflectance values for four wavelengths recommended by the Commission on Ore Microscopy of the International Mineralogical Association are given in bold type.

Wavelength, nm	R_1	R_2
400	17.3	16.8
420	16.8	16.4
440	16.4	16.0
460	16.0	15.5
470	**15.8**	**15.3**
480	15.6	15.2
500	15.3	15.0
520	15.3	14.8
540	15.0	14.7
546	**15.0**	**14.7**
560	15.0	14.6
580	14.9	14.6
589	**14.9**	**14.5**
600	14.8	14.5
620	14.8	14.5
640	14.8	14.4
650	**14.8**	**14.4**
660	14.8	14.4
680	14.7	14.4
700	14.7	14.3

3.4. Chemical Composition

Chemical data for nöggerathite-(Ce) are given in Table 3. Contents of other elements with atomic numbers >8 are below detection limits. Based on structural data (see below) and by analogy with laachite [9], iron and manganese are considered as Fe^{2+} and Mn^{2+}, respectively.

Table 3. Chemical data for nöggerathite-(Ce). Upper and lower values for each constituent correspond to the holotype and the cotype, respectively.

Constituent	wt %	Range	Standard Deviation	Standard Used	X-ray Line Measured
CaO	5.45	5.27–5.55	0.10	Wollastonite	K
	5.29	5.12–5.39	0.34		
MnO	4.19	4.07–4.32	0.09	$MnTiO_3$	K
	4.16	4.06–4.34	0.13		
FeO	7.63	7.46–7.79	0.14	Fe	K
	6.62	6.23–6.83	0.28		
Al_2O_3	0.27	0.18–0.38	0.07	Albite	K
	0.59	0.48–0.78	0.14		
Y_2O_3	0.00	–	–	YPO_4	L
	0.90	0.61–0.99	0.16		
La_2O_3	3.17	3.05–3.28	0.10	$LaPO_4$	L
	3.64	3.47–3.84	0.16		
Ce_2O_3	11.48	11.27–11.73	0.19	$CePO_4$	L
	11.22	10.95–11.69	0.33		
Pr_2O_3	1.04	0.89–1.24	0.12	$PrPO_4$	L
	0.92	0.90–0.97	0.03		

Table 3. *Cont.*

Constituent	wt %	Range	Standard Deviation	Standard Used	X-ray Line Measured
Nd_2O_3	2.18 2.46	2.10–2.34 2.28–2.81	0.08 0.25	$NdPO_4$	L
ThO_2	2.32 1.98	2.11–2.50 1.79–2.17	0.15 0.16	ThO_2	M
TiO_2	17.78 18.69	17.45–18.12 18.49–18.90	0.27 0.16	TiO_2	M
ZrO_2	27.01 27.69	26.82–27.26 27.51–27.86	0.19 0.11	ZrO_2	L
Nb_2O_5	17.04 15.77	16.72–17.37 15.53–15.99	0.28 0.19	$LiNbO_3$	L
Total	99.59 99.82	-	-	-	-

The empirical formulae (based on 14 O *apfu*) are: $(Ce_{0.59}La_{0.165}Nd_{0.11}Pr_{0.05})_{\Sigma 0.915}Ca_{0.82}Th_{0.07}Mn_{0.50}Fe_{0.90}Al_{0.045}Zr_{1.86}Ti_{1.88}Nb_{1.07}O_{14}$ (holotype) and $(Ce_{0.57}La_{0.19}Nd_{0.12}Pr_{0.05}Y_{0.06})_{\Sigma 0.99}Ca_{0.79}Th_{0.06}Mn_{0.49}Fe_{0.77}Al_{0.10}Zr_{1.89}Ti_{1.96}Nb_{1.00}O_{14}$ (cotype).

The simplified formula is $(Ce,Ca)_2Zr_2(Nb,Ti)(Ti,Nb)_2Fe^{2+}O_{14}$.

3.5. X-ray Diffraction Data and Crystal Structure

Powder X-ray diffraction data are presented in Table 4. Diffraction peaks are readily indexed in the orthorhombic unit cell, space group *Cmca*. The unit cell parameters calculated from the powder data are: a = 7.296(1), b = 14.147(2), c = 10.161(1) Å, and V = 1048.9(2) Å^3.

Table 4. Powder X-ray diffraction data for the holotype specimen of nöggerathite-(Ce).

I_{obs}, %	d_{obs}, Å	I_{calc}, %	d_{calc}, Å	h	k	l	I_{obs}, %	d_{obs}, Å	I_{calc}, %	d_{calc}, Å	h	k	l
4	7.068	2	7.074	0	2	0	2	1.743	1	1.743	3	1	4
2	5.806	1	5.805	0	2	1	-	-	1	1.742	0	8	1
3	5.463	1	5.466	1	1	1	1	1.735	1	1.734	3	5	2
5	5.085	1	5.081	0	0	2	1	1.721	1	1.722	2	2	5
1	4.131	1	4.126	0	2	2	1	1.710	1	1.709	2	6	3
2	4.001	2	3.999	1	1	2	4	1.690	3	1.688	1	7	3
10	3.689	8	3.690	1	3	1	1	1.667	1	1.668	4	2	2
2	3.536	1	3.537	0	4	0	2	1.646	1	1.647	0	2	6
3	3.343	2	3.340	0	4	1	-	-	1	1.646	3	3	4
2	3.238	1	3.242	2	2	0	-	-	1	1.639	1	1	6
91	**2.963**	100	2.963	2	0	2	1	1.600	1	1.601	4	4	1
100	**2.903**	93	2.903	0	4	2	2	1.571	1	1.572	2	8	1
2	2.731	1	2.733	2	2	2	-	-	1	1.568	0	8	3
2	2.575	1	2.574	1	3	3	1	1.561	1	1.562	2	6	4
39	**2.540**	14	2.540	0	0	4	**20**	**1.543**	20	1.544	4	4	2
-	-	27	2.539	2	4	0	10	1.532	2	1.536	3	7	1
1	2.393	1	2.391	0	2	4	-	-	10	1.536	2	0	6
1	2.367	1	2.365	1	1	4	-	-	11	1.527	0	4	6
5	2.343	5	2.342	2	2	3	**16**	**1.519**	17	1.519	2	8	2
-	-	1	2.341	1	5	2	1	1.500	1	1.501	2	2	6
3	2.298	3	2.297	0	6	1	1	1.494	1	1.492	3	5	4
1	2.270	1	2.271	2	4	2	6	1.482	6	1.482	4	0	4
3	2.166	2	2.168	3	1	2	-	-	1	1.481	3	3	5
1	2.139	1	2.138	1	3	4	6	1.451	6	1.451	0	8	4
1	2.113	1	2.114	3	3	1	1	1.441	1	1.440	2	8	3
2	2.082	1	2.081	1	5	3	1	1.427	1	1.428	4	6	1
1	2.062	1	2.063	0	4	4	-	-	1	1.425	1	5	6
1	2.033	1	2.032	2	4	3	3	1.413	2	1.413	3	7	3
1	2.001	1	2.000	2	2	4	2	1.407	1	1.406	1	7	5
3	1.956	2	1.957	3	1	3	1	1.400	1	1.399	1	9	3
-	-	1	1.953	0	2	5	1	1.381	1	1.381	5	3	1

Table 4. *Cont.*

I_{obs}, %	d_{obs}, Å	I_{calc}, %	d_{calc}, Å	*h*	*k*	*l*	I_{obs}, %	d_{obs}, Å	I_{calc}, %	d_{calc}, Å	*h*	*k*	*l*
3	1.940	1	1.944	2	6	1	1	1.365	1	1.367	4	4	4
-	-	1	1.935	0	6	3	-	-	1	1.363	1	3	7
6	1.914	3	1.913	1	7	1	1	1.334	1	1.334	5	1	3
1	1.847	1	1.845	2	6	2	-	-	1	1.334	0	8	5
-	-	1	1.830	1	5	4	-	-	1	1.333	4	2	5
15	**1.823**	15	1.824	4	0	0	-	-	1	1.333	3	3	6
-	-	1	1.822	3	3	3	1	1.307	1	1.309	3	9	1
51	**1.796**	56	1.796	2	4	4	-	-	1	1.305	0	10	3
10	1.769	12	1.768	0	8	0	1	1.288	1	1.289	5	3	3

Note: The d_{calc} values are calculated for unit cell parameters obtained from single-crystal data.

The crystal structure of the holotype sample (see Tables 5–7) was solved by direct methods based on single-crystal X-ray diffraction data and refined to R = 0.0198 for 574 unique reflections with $I > 2\sigma(I)$. Nöggerathite-(Ce) is orthorhombic, with space group *Cmca*. The refined unit cell parameters are: a = 7.2985(3), b = 14.1454(4), c = 10.1607(4) Å, V = 1048.99(7) Å^3; and Z = 4.

Solving the crystal structure of nöggerathite-(Ce) reveals the alternation of two types of bent polyhedral layers, namely an octahedral layer (Figure 4A) and a layer of cations with seven- and eight-fold coordination (Figure 4B). The octahedral layer is built by vertex-sharing $M(3)O_6$ and $M(4)O_6$ octahedra forming three- and six-membered rings, whereas $M(5)$ and $M(6)$ sites are located in the centers of six-membered rings. The adjacent sites $M(5)$ and $M(6)$, with coordination numbers 4 and 5, respectively, are statistically occupied and contain Fe^{2+} as the major cation (Figure 4C). The $M(1)$-centered polyhedron is a distorted cube which shares edges with neighboring $M(1)$-centered cubes to form rows along the a axis. Similar rows are formed by seven-fold $M(2)$-centered polyhedra (mono-capped octahedra). Adjacent rows of eight- and seven-fold polyhedra are linked with each other via common edges forming a dense layer. A general view of the crystal structure of nöggerathite-(Ce) is shown in Figure 5.

The refined crystal/chemical formula of nöggerathite-(Ce) is as follows (Z = 4, *REE* are modeled by Ce, coordination numbers of cations are indicated with Roman numerals): $^{VIII}(LREE_{0.88}Ca_{0.80}Mn_{0.24}Th_{0.08})$ $^{VII}(Zr_{1.88}Mn_{0.12})^{VI}(Nb_{1.22}Ti_{0.78})^{VI}(Ti_{1.48}Nb_{0.48}Al_{0.04})^{IV}(Fe_{0.48}Mn_{0.08})^{V}(Fe_{0.40}Mn_{0.04})_2O_{14}$.

Table 5. Atom coordinates, equivalent thermal displacement parameters (U_{eq}, Å^2), site populations and site multiplicities (Q) in the structure of nöggerathite-(Ce).

Site	*x*	*y*	*z*	U_{eq}	Site Population	*Q*
$^{VIII}M(1)$	0.25	0.11753(3)	–0.2500	0.00954(18)	$Ce_{0.44}Ca_{0.40}Mn_{0.12}Th_{0.04}$	8
$^{VII}M(2)$	0.5	0.23411(4)	0.01426(5)	0.0120(2)	$Zr_{0.937(9)}Mn_{0.063(9)}$	8
$^{VI}M(3)$	0.0	0.0	0.0	0.0112(3)	$Nb_{0.608(8)}Ti_{0.392(8)}$	4
$^{VI}M(4)$	0.25	0.13297(5)	0.25	0.0129(2)	$Ti_{0.74}Nb_{0.24}Al_{0.02}$	8
$^{IV}M(5)$	0.4211(8)	0.0	0.0	0.0301(9)	$Fe_{0.24}Mn_{0.04}$	8
$^{V}M(6)$	0.5	0.0140(5)	0.0342(9)	0.0393(19)	$Fe_{0.20}Mn_{0.02}$	8
O(1)	0.1948(4)	0.03150(18)	0.1256(2)	0.0236(6)	O	16
O(2)	0.2131(4)	0.23287(17)	0.1201(2)	0.0218(6)	O	16
O(3)	0.5	0.1081(2)	–0.1007(4)	0.0182(8)	O	8
O(4)	0.0	0.1288(2)	–0.0912(4)	0.0184(8)	O	8
O(5)	0.5	0.1366(3)	0.1756(4)	0.0250(9)	O	8

Table 6. Selected interatomic distances (Å) in the structure of nöggerathite-(Ce).

Cation	Ligand	Distance	Cation	Ligand	Distance
$M(1)$	O(3)	2.376(2) × 2	$M(3)$	O(4)	2.044(3) × 2
$M(1)$	O(4)	2.441(3) × 2	$M(4)$	O(2)	1.952(2) × 2
$M(1)$	O(1)	2.491(3) × 2	$M(4)$	O(1)	1.955(3) × 2
$M(1)$	O(2)	2.508(3) × 2	$M(4)$	O(5)	1.9759(16) × 2
$M(2)$	O(4)	2.091(3)	$M(5)$	O(3)	1.928(4) × 2

Table 6. *Cont.*

Cation	Ligand	Distance	Cation	Ligand	Distance
M(2)	O(2)	2.122(3) × 2	*M*(5)	O(1)	2.134(5) × 2
M(2)	O(3)	2.132(4)	*M*(6)	O(3)	1.855(8)
M(2)	O(5)	2.142(4)	*M*(6)	O(3)	1.910(9)
M(2)	O(2)	2.354(3) × 2	*M*(6)	O(5)	2.251(9)
M(3)	O(1)	1.961(3) × 4	*M*(6)	O(1)	2.426(5) × 2

Table 7. Cation distribution in structurally investigated samples of zirconolite-3*O*, laachite, and nöggerathite-(Ce).

Site	Zirconolite-3*O*	Laachite	Nöggerathite-(Ce)
$^{VIII}M(1)$	$Ca_{0.53}Ce_{0.41}Na_{0.04}Th_{0.02}$	$Ca_{0.28}Mn_{0.26}Ln_{0.26}Th_{0.14}Y_{0.06}$ $Ca_{0.32}Mn_{0.28}Ln_{0.24}Th_{0.14}Y_{0.02}$	$Ln_{0.44}Ca_{0.40}Mn_{0.12}Th_{0.04}$
$^{VII}M(2)$	Zr	$Zr_{0.78}Mn_{0.22}$	$Zr_{0.937}Mn_{0.063}$
$^{VI}M(3)$	$Ti_{0.52}Nb_{0.47}Ta_{0.01}$	$Nb_{0.82}Ti_{0.18}$	$Nb_{0.608}Ti_{0.392}$
$^{VI}M(4)$	$Ti_{0.88}Nb_{0.12}$	$Ti_{0.72}Nb_{0.28}$ $Nb_{0.44}Ti_{0.40}Al_{0.16}$	$Ti_{0.74}Nb_{0.24}Al_{0.02}$
$^{IV}M(5)$	$Fe_{0.46}$	$Fe_{0.34}Mn_{0.10}Y_{0.06}$	$Fe_{0.24}Mn_{0.04}$
$^{V}M(6)$	$Fe_{0.03}$		$Fe_{0.20}Mn_{0.02}$
Reference	[16]	[9]	This work

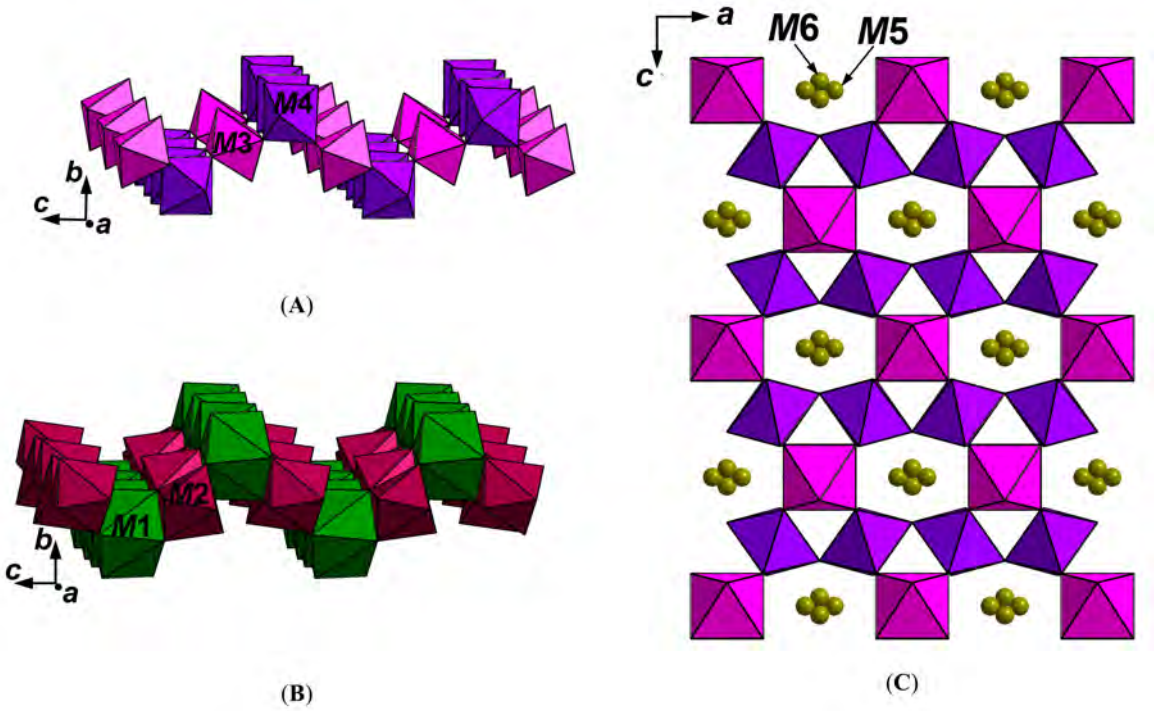

Figure 4. Octahedral (**A**) and large-cation (**B**) layers and arrangement of Fe-dominant sites *M*(5) and *M*(6) inside the octahedral layer (**C**) in the structure of nöggerathite-(Ce).

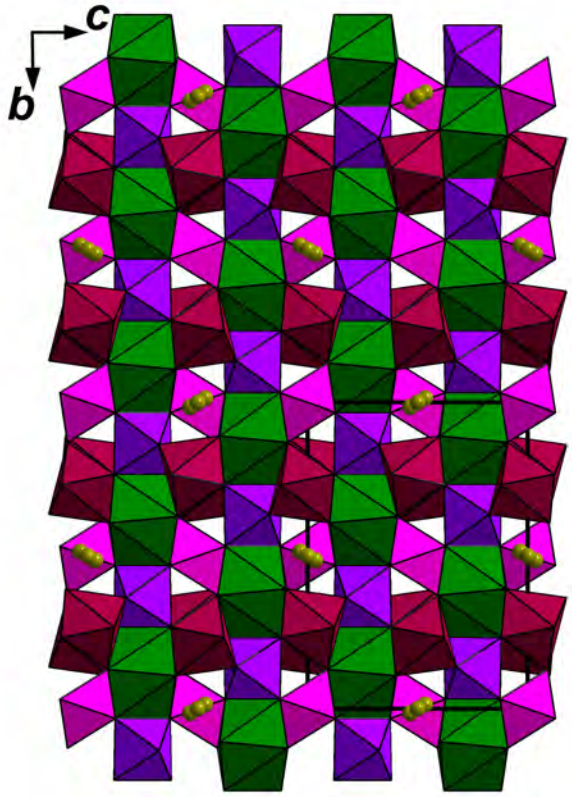

Figure 5. The crystal structure of nöggerathite-(Ce). The unit cell is outlined. For legend see Figure 4.

4. Discussion

Nöggerathite-(Ce) is isostructural with zirconolite-3*O* and is its *REE*-dominant analogue, with Nb prevailing in one of two octahedral sites (see Tables 5–7). Zirconolite-3*O* was originally described as "polymignite" [17,18] and was later redefined and renamed [16,19–21]. However, "polymignite" is usually metamict and, as a rule, its powder X-ray diffraction pattern can be obtained only after calcination.

Unlike most samples of zirconolites, nöggerathite-(Ce) is non-metamict because it was formed recently: the last eruption of the Laach Lake volcano occurred no later than 13,000 years ago. According to Schmitt [14], the age of zircon from sanidinitic ejecta of the Laach Lake volcano is between 17,000 and 30,000 years. Consequently, sanidinite could have formed 4000–17,000 years before the eruption.

A non-metamict *REE*-, Nb-, and Mn-rich variety (or, in accordance with the accepted mineralogical nomenclature rules, an *REE*-analogue) of zirconolite-3*O* from the Laach Lake eruptive center was described by Della Ventura et al. [7] without structural data. Its chemical composition is close to that of nöggerathite-(Ce) and varies within the following ranges (calculated on the basis of 7 O *apfu*): $Ca_{0.312\text{-}0.337}Y_{0.079\text{-}0.093}La_{0.069\text{-}0.086}Ce_{0.269\text{-}0.296}Pr_{0.020\text{-}0.028}Nd_{0.052\text{-}0.062}Sm_{0.004\text{-}0.006}Gd_{0.005\text{-}0.006}Dy_{0.003\text{-}0.006}Er_{0.003\text{-}0.005}Th_{0.014\text{-}0.073}U_{0.008\text{-}0.022}Mn_{0.345\text{-}0.397}Mg_{0.003\text{-}0.005}Al_{0.020\text{-}0.025}Fe_{0.301\text{-}0.339}Zr_{0.888\text{-}0.910}Hf_{0.006\text{-}0.009}Ti_{0.840\text{-}0.888}Nb_{0.575\text{-}0.613}Ta_{0.007\text{-}0.009}Si_{0.000\text{-}0.012}O_{7.000}$.

The empirical formula corresponding to spot analysis number 1 from [7], calculated on 14 O *apfu*, is $(Ln_{0.98}Ca_{0.63}Mn_{0.17}Y_{0.16}Th_{0.04}U_{0.02})_{\Sigma 2.00}[(Fe_{0.65}Mn_{0.55}Al_{0.05}Mg_{0.01})(Zr_{1.79}Hf_{0.01})(Ti_{1.71}Nb_{1.19}Ta_{0.02})Si_{0.02}]_{\Sigma 6.00}O_{14}$. The latter formula may correspond to nöggerathite-(Ce) or its Mn-dominant analogue (with Mn > Fe in the *M*(5) and *M*(6) sites).

Another crystalline mineral related to zirconolite-3*O* and nöggerathite-(Ce) is laachite ($Ca_2Zr_2Nb_2TiFeO_{14}$), which originates from sanidinite of the Laach Lake volcano and demonstrates a perfect crystal structure. Laachite is a monoclinic (pseudo-orthorhombic) analogue of zirconolite-3*O*, with Nb prevailing over Ti in two octahedral sites [9]. Chemical compositions of 24 samples of

zirconolite-type minerals from the Laach Lake volcano have been determined by us. Most of them correspond to stefanweissite $(Ca,REE)_2Zr_2(Nb,Ti)(Ti,Nb)_2Fe^{2+}O_{14}$ (IMA 2018-020), which is an analogue of zirconolite-3*O* with Nb as a species-defining component. Comparative data for nöggerathite-(Ce), zirconolite-3*O*, and laachite are given in Table 8 and in Figures 6–8. The main substitution scheme following from the compositional data for these minerals is: $Ca^{2+} + Ti^{4+} + Zr^{4+} \leftrightarrow REE^{3+} + Nb^{5+} + Mn^{2+}$. However, as one can see from Figure 7, the substitution Zr^{4+} for Mn^{2+} in the *M*(2) site is to be completed with other (subordinate) schemes involving zirconium, most probably $Zr^{4+} \leftrightarrow Ti^{4+}$ and/or $REE^{3+} + Zr^{4+} \leftrightarrow Ca^{2+} + Nb^{5+}$.

Table 8. Comparative data for nöggerathite-(Ce) and related minerals.

Mineral	Nöggerathite-(Ce)	Laachite	Zirconolite-3*O*
Idealized formula	$(Ce,Ca)_2Zr_2(Nb,Ti)(Ti,Nb)_2Fe^{2+}O_{14}$	$Ca_2Zr_2Nb_2TiFeO_{14}$	$CaZrTi_2O_7$
Crystal system	Orthorhombic	Monoclinic	Orthorhombic
Space group	*Cmca*	*C*2/*c*	*Cmca*
a, Å	7.2985	7.3119	7.278–7.284
b, Å	14.1454	14.1790	14.147–14.18
c, Å	10.1607	10.1700	10.145–10.148
β, °	90	90.072	90
Z	4	4	8
Strong lines of the X-ray powder diffraction pattern: *d*, Å (*I*, %)	2.963 (91) 2.903 (100) 2.540 (39) 1.823 (15) 1.796 (51) 1.543 (20) 1.519 (16)	4.298 (22) 2.967 (100) 2.901 (59) 2.551 (32) 1.800 (34) 1.541 (24) 1.535 (23) 1.529 (23)	3.176 (30) 2.914 (100) 2.506 (40) 1.980 (90) 1.792 (90) 1.517 (10)
Refractive index	2.267 (mean, calc.)	2.26 (mean, calc.)	2.215 (meas., metamict); 2.26–2.31 (calc.)
Density, g cm^{-3}	5.332 (calc.)	5.42 (calc.)	4.7 (meas.) 4.9 (calc.)
Sources	This work	[9]	[7,8,16,19–22]

Note: For zirconolite-3*O* the standard space group *Cmca* is given instead of the space group *Acam* reported in earlier publications.

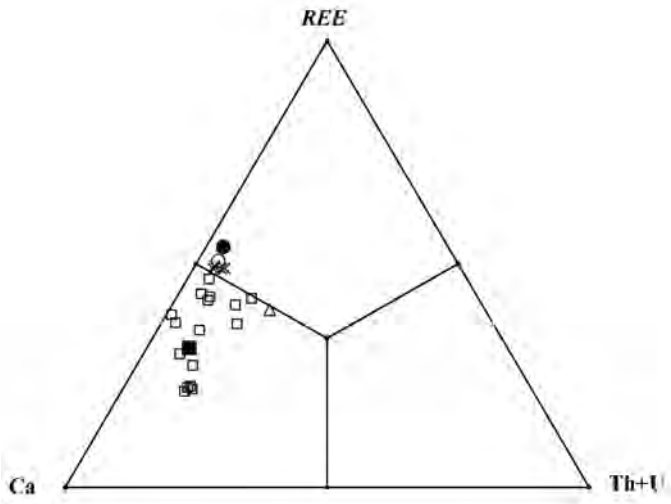

Figure 6. Ratios of large cations with coordination number 8 in zirconolite-type minerals from the Laach Lake volcano: the holotype (○) and cotype (●) nöggerathite-(Ce), other nöggerathite-(Ce) samples (×), the stefanweissite holotype (■), other stefanweissite samples (□), and the holotype laachite (Δ).

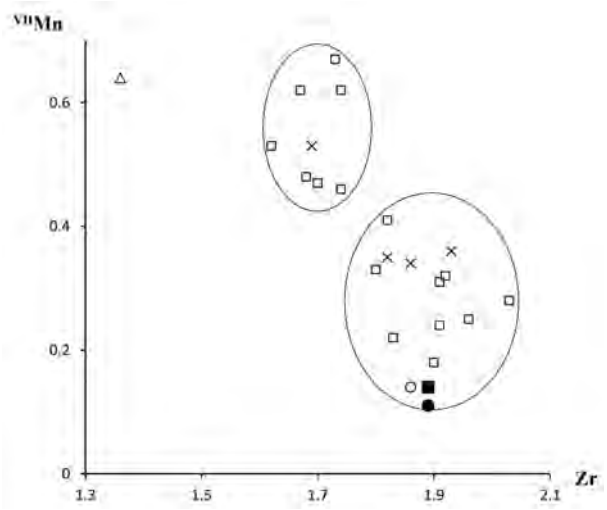

Figure 7. The relationships between the Zr and Mn contents (*apfu*) at the *M*(2) site of zirconolite-type minerals from the Laach Lake volcano. The correlation coefficient is $R = -0.757$ for the whole set of analyses, but almost no correlation is observed within Zr-rich (i.e., Mn-poor) and Zr-poor (i.e., Mn-rich) groups of samples separated with ellipses. For legend see Figure 6.

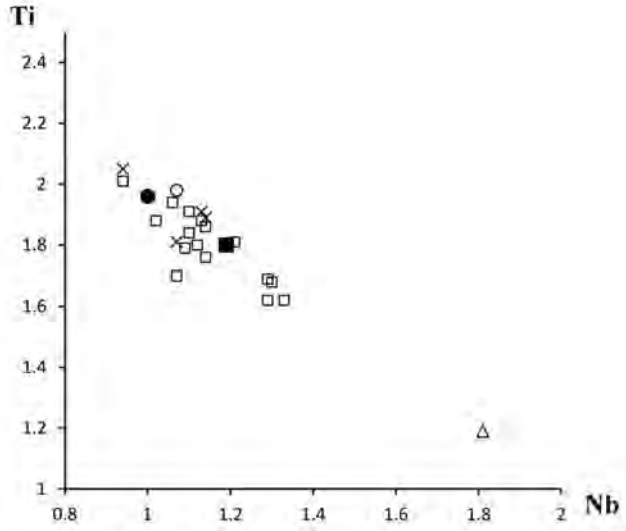

Figure 8. Correlation between contents of Ti and Nb (*apfu*) in zirconolite-type minerals from the Laach Lake volcano. Correlation coefficient $R = -0.932$. For legend see Figure 6.

REE-dominant zirconolite-type minerals (with *REE* > Ca in atomic units and Y prevailing among rare-earth elements) have been described in gabbro pegmatite in St. Kilda, Scotland, United Kingdom, in nepheline syenite from Tchivera, Angola, in metamorphic rocks of the Vestfold Hills, East Antarctica, and in lunar rocks [6], but crystal structures of these minerals have not been studied because of their metamict state.

An important specific feature of nöggerathite-(Ce) is its high content of niobium. A review of localities of zirconolites worldwide and a compilation of chemical compositions of about 300 samples were provided by Williams and Gieré [6]. All analyses show significant predominance of Ti over Nb. For most samples the content of Nb_2O_5 is below 10 wt %. The Nb-richest zirconolite from Vuoriyarvi, Northern Karelia, Russia, was described by Borodin et al. [23] as "niobozirconolite". It contains 0.798 Nb atoms and 1.081 Ti atoms as per a formula calculated on the basis of 7 O atoms. High content of Nb was also detected in zirconolite samples from Kovdor, Kola, Russia (0.652 *apfu* Nb vs. 0.857 *apfu* Ti), Kaiserstuhl, Germany (0.687 *apfu* Nb vs. 0.702 *apfu* Ti), and Sokli, Finland (0.608 *apfu* Nb vs. 0.773 *apfu* Ti) [6].

Author Contributions: N.V.C., N.V.Z., and I.V.P. wrote the paper. C.S. collected the type material. B.T. and W.S. collected other samples of zirconolite-type minerals. S.N.B. obtained single-crystal X-ray diffraction data. N.V.Z. and D.Y.P. solved and refined the crystal structure. I.V.P. obtained powder X-ray diffraction data. V.N.E. and N.V.C. conceived and designed chemical data. M.F.V. obtained Raman spectra. N.V.C. analyzed Raman data. Y.S.P. measured reflectance data and hardness.

Funding: This research was funded by the Russian Science Foundation, under grant no. 14-17-00048 (for part of the chemical study of nöggerathite-(Ce) and other zirconolite-type minerals) and the Russian Foundation for Basic Research, under grant no. 18-29-12007 (for parts of the mineralogical study, Raman spectroscopy and X-ray structural analysis). SNB acknowledges St. Petersburg State University for financial support, grant no. 3.42.741.2017 (in part of single-crystal measurements).

Acknowledgments: The authors thank the X-ray Diffraction Centre of St. Petersburg State University for instrumental and computational resources.

Conflicts of Interest: The authors declare no conflict of interest.

References

1. Ringwood, A.E.; Kelly, P.M. Immobilization of high-level waste in ceramic waste forms. *Philos. Trans. R. Soc. A* **1986**, *319*, 63–82. [CrossRef]
2. Donald, I.W.; Metcalfe, B.L.; Taylor, R.N.J. The immobilization of high level radioactive wastes using ceramics and glasses. *J. Mater. Sci.* **1997**, *32*, 5851–5887. [CrossRef]
3. Laverov, N.P.; Yudintsev, S.V.; Stefanovsky, S.V.; Omel'yanenko, B.I.; Nikonov, B.S. Murataite as a universal matrix for immobilization of actinides. *Geol. Ore Depos.* **2006**, *48*, 335–356. [CrossRef]
4. Barinova, T.V.; Borovinskaya, I.P.; Ratnikov, V.I.; Ignat'eva, T.I. Self-propagating high-temperature synthesis for immobilization of high-level waste in mineral-like ceramics: 1. Synthesis and study of titanate ceramics based on perovskite and zirconolite. *Radiochemistry* **2008**, *50*, 316–320. [CrossRef]
5. Zhang, Y.; Gregg, D.J.; Kong, L.; Jovanovich, M.; Triani, G. Zirconolite glass-ceramics for plutonium immobilization: The effects of processing redox conditions on charge compensation and durability. *J. Nucl. Mater.* **2017**, *490*, 238–241. [CrossRef]
6. Williams, C.T.; Gieré, R. Zirconolite: A review of localities worldwide, and a compilation of its chemical compositions. *Bull. Nat. Hist. Mus. Lond.* **1996**, *52*, 1–24.
7. Della Ventura, G.; Bellatreccia, F.; Williams, C.T. Zirconolite with significant REEZrNb(Mn,Fe)O7 from a xenolith of the Laacher See eruptive center, Eifel volcanic region, Germany. *Can. Mineral.* **2000**, *38*, 57–65. [CrossRef]
8. Sinclair, W.; Eggleton, R.A. Structure refinement of zirkelite (zirconolite) from Kaiserstuhl, Germany. *Am. Mineral.* **1982**, *67*, 615–620.
9. Chukanov, N.V.; Krivovichev, S.V.; Pakhomova, A.S.; Pekov, I.V.; Schäfer, Ch.; Vigasina, M.F.; Van, K.V. Laachite, $(Ca,Mn)_2Zr_2Nb_2TiFeO_{14}$, a new zirconolite-related mineral from the Eifel volcanic region, Germany. *Eur. J. Mineral.* **2014**, *26*, 103–111. [CrossRef]
10. Zubkova, N.V.; Chukanov, N.V.; Pekov, I.V.; Ternes, B.; Schüller, W.; Pushcharovsky, D.Y. The crystal structure of natural nonmetamict Nb-rich zirconolite-3T from the Eifel paleovolcanic region, Germany. *Z. Kristallogr.* **2018**, *233*. [CrossRef]
11. Litt, T.; Brauer, A.; Goslar, T.; Merk, J.; Balaga, K.; Mueller, H.; Ralska-Jasiewiczowa, M.; Stebich, M.; Negendank, J.F.W. Correlation and synchronisation of Lateglacial continental sequences in northern Central Europe based on annually laminated lacustrine sediments. *Quat. Sci. Rev.* **2001**, *20*, 1233–1249. [CrossRef]
12. Schmitt, A.K.; Wetzel, F.; Cooper, K.M.; Zou, H.; Wörner, G. Magmatic longevity of Laacher See volcano (Eifel, Germany) indicated by U–Th dating of intrusive carbonatites. *J. Petrol.* **2010**, *51*, 1053–1085. [CrossRef]
13. Frechen, J. Vorgänge der Sanidinit-Bildung im Laacher Seegebiet. *Fortschritte der Mineralogie* **1947**, *26*, 147–166. (In German)
14. Schmitt, A.K. Laacher See revisited: High-spatial-resolution zircon dating indicates rapid formation of a zoned magma chamber. *Geology* **2006**, *34*, 597–600. [CrossRef]
15. Britvin, S.N.; Dolivo-Dobrovolsky, D.V.; Krzhizhanovskaya, M.G. Software for processing the X-ray powder diffraction data obtained from the curved image plate detector of Rigaku RAXIS Rapid II diffractometer. *Zap. Ross. Mineral. Obsh.* **2017**, *146*, 104–107. (In Russian)

16. Mazzi, F.; Munno, R. Calciobetafite (new mineral of the pyrochlore group) and related minerals from Campi Flegrei, Italy; crystal structures of polymignite and zirkelite: Comparison with pyrochlore and zirconolite. *Am. Mineral.* **1983**, *68*, 262–276.
17. Berzelius, J. Undersökning af några Mineralier. 2. Polymignit. *Kongl. Svenska Vetensk.-Acad. Handl.* **1984**, 338–345. (In Swedish)
18. Brøgger, W.C. Die Mineralien der Syenitpegmatitgänge der südnorwegischen Augit und Nephelinsyenite. *Z. Kristallogr. Speziellen Teil* **1890**, *16*, 1–663. (In German)
19. Bayliss, P.; Mazzi, F.; Munno, R.; White, T.J. Mineral nomenclature: Zirconolite. *Mineral. Mag.* **1989**, *53*, 565–569. [CrossRef]
20. Chukhrov, F.V.; Bonshtedt-Kupletskaya, E.M. *Mineraly Vol. II(3)*; Nauka: Moscow, Russia, 1967; pp. 188–190. (In Russian)
21. Pudovkina, Z.V.; Chernitzova, N.M.; Pyatenko, Y.A. Crystallographic study of polymignite. *Zap. Vses. Mineral. Obshch.* **1969**, *98*, 193–199. (In Russian)
22. Borodin, L.S.; Nazarenko, I.I.; Richter, T.L. On a new mineral zirconolite–A complex oxide of AB_3O_7 type. *Dokl. Akad. Nauk SSSR* **1956**, *110*, 845–848. (In Russian)
23. Borodin, L.S.; Bykova, A.V.; Kapitonova, T.A.; Pyatenko, Y.A. New data on zirconolite and its new niobian variety. *Dokl. Akad. Nauk SSSR* **1960**, *134*, 1188–1192. (In Russian)